



Enhancing the UV/heat stability of LLDPE irrigation pipes via different stabilizer formulations

Athanasios D. Porfyris¹  | Adriaan S. Luyt²  | Soumia Gasmi² | Sarah S. Malik² | Reem M. Aljindi^{2,3} | Mabrouk Ouederni⁴ | Stamatina N. Vouyiouka¹ | Rudolf Pfaendner⁵ | Constantine D. Papaspyrides¹

¹Laboratory of Polymer Technology, School of Chemical Engineering, National Technical University of Athens, Athens, Greece

²Center for Advanced Materials, Qatar University, Doha, Qatar

³Department of Mechanical & Industrial Engineering, College of Engineering, Qatar University, Doha, Qatar

⁴Qatar Petrochemical Company (QAPCO), Doha, Qatar

⁵Fraunhofer Institute for Structural Durability and System Reliability LBF, Darmstadt, Germany

Correspondence

Athanasios D. Porfyris, Laboratory of Polymer Technology, School of Chemical Engineering, National Technical University of Athens, Zographou Campus, 157 80 Athens, Greece.
Email: adporfyris@mail.ntua.gr

Funding information

Qatar National Research Fund, Grant/Award Number: NPRP 9-161-1-030

Abstract

Herein different stabilizer formulations of linear low-density polyethylene (LLDPE) against UV- and heat-initiated degradation are described. The project aims at outdoor applications, such as irrigation piping and profiles, in the Middle East desert regions, where long-term weathering stability due to high temperatures and solar radiation is important. Two UV/heat formulations, without and with carbon black (CB) as pigment, were incorporated into LLDPE by melt compounding. Neat LLDPE and the stabilized compounds were exposed to accelerated UV and heat aging. Morphological analysis through scanning electron microscopy of the UV-exposed neat LLDPE showed more severe surface cracking compared to the CB-containing LLDPE, while all stabilized compounds did not show any surface degradation. Crack formation was less visible for the thermally aged samples. A significant decrease in molecular weight (MW) was observed for the neat UV-exposed LLDPE, while both unpigmented stabilized compounds showed little change in MW. Mechanical properties, thermal analysis, and carbonyl index results supported the morphological results, which confirmed that CB alone was slightly more effective in protecting the LLDPE against UV initiated degradation, but performed worse against thermal initiated degradation. UV1 and UV2 compounds were efficient against both UV- and heat-initiated degradation, with UV1 performing better for unpigmented compounds, and UV2 for the pigmented ones.

KEYWORDS

accelerated thermal aging, artificial weathering, linear low-density polyethylene, mechanical properties, surface morphology, thermal properties, UV/heat stabilization

1 | INTRODUCTION

Polyethylenes (PEs) are the most widely used polymers because of their good processability, low cost, and chemical and mechanical resistance. The consumption of PEs

has reached 170 million tons in 2018, and the Middle East has been reported to be the second fastest growing PE market worldwide.^[1–3] PEs are widely used for various outdoor applications such as irrigation pipes, automotive parts, building pipes, agricultural ground cover,

This is an open access article under the terms of the Creative Commons Attribution License, which permits use, distribution and reproduction in any medium, provided the original work is properly cited.

© 2021 The Authors. *SPE Polymers* published by Wiley Periodicals LLC on behalf of Society of Plastics Engineers.

storage tanks, and wire and cable insulation. Despite the good properties of PEs, their lifetime is reduced as a result of a significant loss in mechanical strength and physical properties because of the continuous exposure to harsh climatic conditions.^[4–10] Indicatively, in Qatar, there are kilometers of carbon black (CB) pigmented PE pipes that are replaced every 6 months due to their degradation as a result of UV radiation, extensive heat, and high humidity.^[11] Replacing these PE pipes is expensive, and disposal of the used pipes adds to the already serious environmental problem, especially since Qatar is considered as one of the world's largest producers of landfills.^[11]

In order to inhibit UV- and heat-induced degradation and to valorize these commodity polymers, by expanding their service lifetime, compounding with additives such as hindered amine light stabilizers (HALS) and UV absorbers (UV-A) is mandatory. The performance of these additives on the polymers' UV and thermal stability can be monitored by accelerated artificial weathering.^[4] The weathering of linear low-density polyethylene (LLDPE) has been studied extensively for a number of applications. Neat polymers,^[9,12] as well as the effect of different additives on the thermal and UV stability of the polymers, were studied.^[13,14] Neat LLDPE samples experienced up to 60% reduction in different mechanical properties after 6 months of outdoor weathering.^[12] On the contrary, PE compounds containing various HALS additives based on tertamethylpiperidine or alkyl substituted N-tertamethylpiperidinemethyl-tetramethyl units, successfully restricted the photodegradation process. HALS are reported as light and long-term thermal stabilizers which have the ability to scavenge radicals created by UV absorption during the photo-oxidation processes by forming nitroxyl radicals through a cyclic mechanism known as the Denisov cycle,^[15] thus they can be regenerated rather than being consumed.^[16] On the other hand, UV-A, one of the most commonly used photo-stabilizers, protect the polymer from photo-oxidation by absorbing the harmful UV radiation (300–400 nm) during the first step of the photo-oxidation process and transform it to heat, thus preventing its interaction with the photoactive chromophoric species in the polymer molecule.^[16,17] Typical examples for UV-A include benzophenone, benzotriazole, cinnamate, and hydroxyphenyl triazine compounds.

The combination of HALS with UV-A reduces the carbonyl index (CI), which is the indicator of the UV and thermal degradation of exposed PEs.^[18] HALS compounds were examined as light stabilizers for LLDPE under natural and artificial weathering with the incorporation level ranging from 0.3 to 0.85 wt%.^[14,16–21] Accelerated weathering tests on multiple LLDPE formulations were conducted. It was observed that PEs, which

contained a combination of HALS and UV-A, showed higher thermal stability and less degradation than those with solely HALS.^[22] On the other hand, a disadvantage of UV-A is that they need a certain absorption depth (sample thickness) to offer a satisfactory level of protection to the polymer.^[23–25] It is however, important to realize that the end application of a PE determines the selection of additives and UV/heat protection formulations.

In the current work, the aim was to establish optimal UV/heat stabilization systems for increasing the service lifetime of LLDPE in thick sections with and without CB through the incorporation of different additives. The concentrations were kept as low as possible so that the pertinent formulations will also be cost-effective. Although the particular field is covered in literature, most publications are related to films, for example, for greenhouses or agricultural uses which is the main application of LLDPE.^[26–28] In addition, the incorporation level of the stabilizers, especially HALS is much higher than the herein applied.^[19–21] Herein the target is to investigate the performance of LLDPE in thick sections, that is, irrigation piping, while also taking CB incorporation and extensive heat stability in consideration, which is quite novel. Moreover, this work is a precursor for examining the performance of the pertinent systems when combined with halogen-free flame-retardants.^[29] In particular, the combination of the two functionalities—flame retardance (FR) and weathering stability—is studied in very few papers on polyolefins and the retention of FR properties after UV exposure consists of a challenge due to the fact that synergistic and/or antagonistic actions can be present.^[30–32] Accordingly, the effect of different HALS and UV-A was herein investigated for LLDPE by means of twin-screw extrusion so as to induce the first functionality of UV stability. The effect of CB on both UV and heat exposure was also systematically studied, since CB constitutes the most common pigment in the manufacture of irrigation pipes. The weathering stability was correlated to the maintenance of mechanical performance, that is, tensile and impact properties, while additional morphological characterization by scanning electron microscopy (SEM), thermal by differential scanning calorimeter (DSC) and thermogravimetric analysis (TGA), and analytical by Fourier transform infrared (FTIR) and gel permeation chromatography (GPC), was performed on all the samples. The investigations aim at the development of sustainable solutions for challenging climate requirements, that is, Middle East desert regions, and to understanding the interactions between the different components necessary for achieving the performance. The most efficient UV/heat formulation was safely identified and proves to be suitable for outdoor irrigation pipes even in the harsh climate conditions of Qatar.

2 | MATERIALS AND METHODS

2.1 | Materials

The polymer that was used in the pertinent work was a linear LLDPE (density = 918 kg/m³, MFI = 1 g/10 min, co-monomer 1-butene, $T_m = 122^\circ\text{C}$). The polymer was provided by Qatar Petrochemical Company (QAPCO, Doha, Qatar) in powdered form and is not prestabilized with antioxidants. Two commercial HALS compounds were used: HALS1: Poly[[6-[(1,1,3,3-tetramethylbutyl)amino]-1,3,5-triazine-2,4-diyl][(2,2,6,6-tetramethyl-4-piperidinyl)imino]-1,6-hexanediy][(2,2,6,6-tetramethyl-4-piperidinyl)imino]], CAS-No. 71878-19-8 (supplied by BASF) and HALS2: N,N',N'',N'''-tetrakis(4,6-bis(butyl-[N-methyl-2,2,6,6-tetramethylpiperidin-4-yl]amino)triazin-2-yl)-4,7-diazadecane-1,10-diamine, CAS-No. 106990-43-6 (supplied by SABO). We also used two UV-A: UV-A1: Methanone, [2-hydroxy-4-(octyloxy)phenyl]phenyl, CAS-No. 1843-05-6 and UV-A2: Phenol, 2-(4,6-Diphenyl-1,3,5-triazin-2-yl)-5-hexyloxy CAS-No. 147315-50-2 (both supplied by BASF). The molecular structures of these compounds are given in Figure 1. Calcium stearate (Ca-St) was used as antiacid and was supplied by Scientific Global Lab Supplies W.L.L., while the CB pigment by Cabot Corporation. To keep the formulation simple no other antioxidant or processing stabilizer was added.

2.2 | Methods

2.2.1 | Sample preparation

The UV/heat stabilization systems were examined in a total content of 0.2 wt% (Table 1) with Ca-St added at 0.05 wt% and an additional 0.3 wt% CB pigment for the pigmented grades. The HALS/UV-A concentration was as low as possible so as to provide the polymer matrix a substantial lifetime extension at an acceptable cost level. The incorporation of the additives was first carried out through thorough 20 min. Bag mixing of the specified amounts of powdered LLDPE and selected additives. Two UV/heat formulations were prepared using these commercial additives. Formulation UV1 combined the most common oligomeric available HALS (HALS1) with a standard benzophenone UV absorber (UV-A1) in loadings of 0.1 wt% each in order to provide a synergistic HALS/UV absorber combination of low cost. The UV2 formulation combined a high-performance HALS consisting of an oligomeric N-methyl-substituted HALS (HALS2), known for its superior performance in the presence of CB,^[15] with a high-performance UV-A of phenyl-triazine type (UV-A2) at levels of 0.1% level each. UV2 formulation was developed as a high-performance alternative, with an inevitable cost increase. Concentrations of the additives were selected to the minimum effective

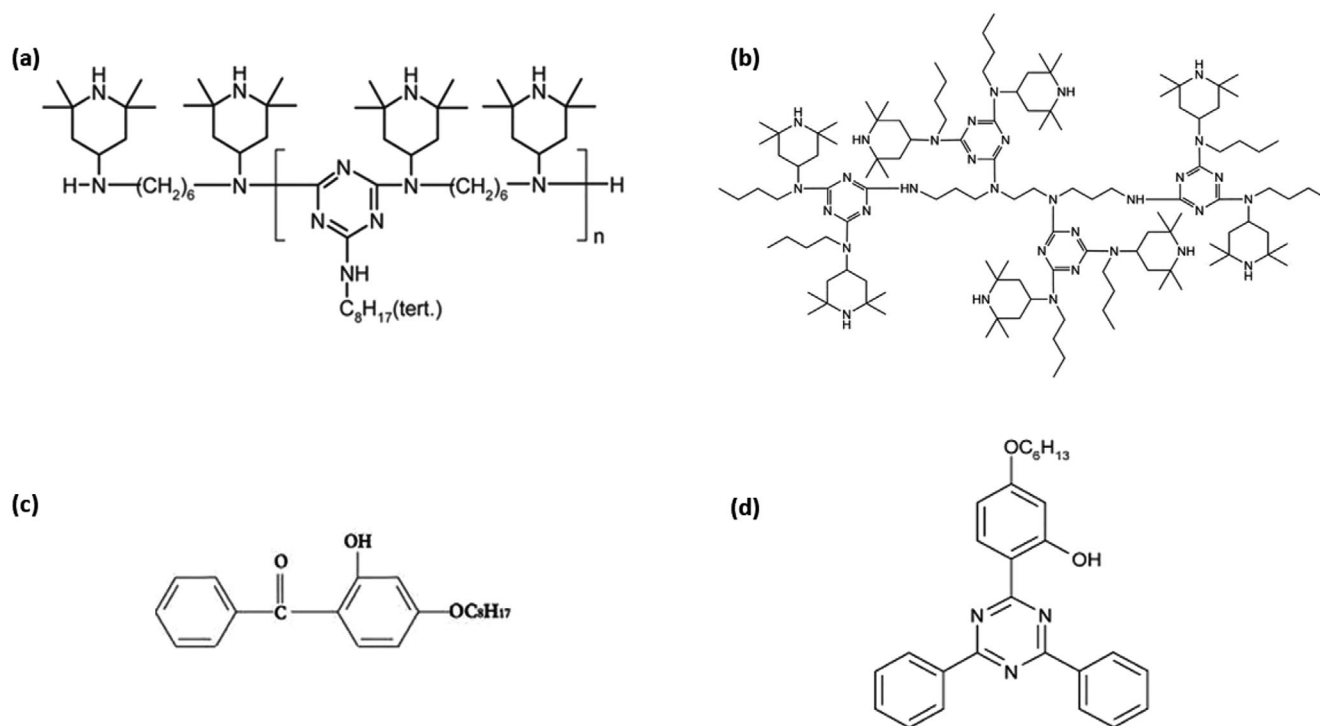


FIGURE 1 Molecular structures of herein used additives. (A) HALS1, (B) HALS2, (C) UV-A1, and (D) UV-A2. HALS, hindered amine light stabilizers; UV-A, UV absorbers

TABLE 1 Compositions of UV/heat formulations in wt%

	LLDPE	HALS1	UV-A1	HALS2	UV-A2	Ca-St	CB
Unpigmented LLDPE							
UV1	99.75	0.1	0.1			0.05	–
UV2	99.75			0.1	0.1	0.05	–
Pigmented LLDPE							
UV1/CB	99.45	0.1	0.1			0.05	0.3
UV2/CB	99.45			0.1	0.1	0.05	0.3

Abbreviations: Ca-St, calcium stearate; CB, carbon black; HALS, hindered amine light stabilizers; LLDPE, linear low-density polyethylene.

level as suggested by the respective technical data sheets (TDS), so as to limit the cost of the formulations.

A twin-screw extruder KETSE 20/40 EC (Model no. 838106) was used to compound the mixed powder at a speed of 90 rpm, and the temperatures of the respective zones from feeder to die were 170–195°C. The extruded mixture was pelletized using a pelletizer to facilitate injection molding. Impact and tensile specimens were prepared by injection molding of the extruded mixture using an ARBURG All-Rounder 570 C injection-molding machine, with temperatures in the range 180–215°C. The impact testing samples were produced with dimensions of 63.5 × 12.7 × 3 mm³ (ASTM D256 standard). The tensile testing samples were injection molded as dumbbell shaped specimens with dimensions 160 × 13 × 3 mm³ (ISO 527 standard).

2.2.2 | Accelerated UV- and heat-aging

The accelerated UV-weathering was performed using an Accelerated Weathering Tester Model QUV-se equipped with solar eye irradiance control and a UV-A lamp. The procedure was based on cycle K references (ISO 4892-3 standard), that are related to Qatar's climatic conditions. The samples were exposed to repetitive cycles of UV exposure and condensation. UV radiation was set for 8 h with an irradiance level of 0.76 W/m² at a wavelength of 340 nm, with a maximum temperature of 60°C. Condensation was then applied for 4 h at a temperature at 50°C. Sampling times applied were 0, 1000, 1500, and 2500 h for all specimens. Reversing of sample sides was performed regularly so that both sides of a sample were equally exposed to the radiation. For example, for a 500 h sample, it was reversed after 250 h, so that each side was exposed to the lamp for 250 h. The same approach was followed for all the sampling times. The actual UV exposure time during the quoted times was shorter (67% of respectively 1000, 1500, and 2500 h), although in this article the terms “weathering time” and “UV exposure time” are used interchangeably as being

the total time the respective samples spent in the weatherometer.

Separate heat aging experiments were conducted in an air circulating oven at 100°C. Dumbbell specimens of each formulation were placed in the oven and the sampling times applied were 1, 2, 3, 4, 6, 9, and 12 months. At each sampling time, five specimens per formulation were removed from the oven and the tensile properties were determined.

2.2.3 | Sample characterization

The tensile properties were measured using a “Lloyd LR50K plus” universal tester according to the ISO 527 standard where no pre-load was applied to the sample. An elongation speed of 10 mm/min and a gage length of 50 mm were used. The Young's modulus (E) was manually calculated from the slope of the stress-strain curve between strain values of 0.2% and 2.2%. Five specimens were tested for each sample. The impact properties of the samples were investigated using an Instron Wolpert PW5 impact tester according to ASTM D256. Specimens with dimensions of 63.5 × 12.7 × 3 mm³ were notched at the center (45° notch and 2 mm depth). The Izod impact strength (in kJ/m²) was calculated according to Equation (1),^[32]

$$a_{iN} = \frac{E_c}{h \times b_N}, \quad (1)$$

where E_c is the corrected measured absorbed energy during impact in J, h is the thickness of the tested specimen in mm and b_N is the remaining width of the tested specimen in mm.

SEM was performed on the surfaces of the injection molded tensile testing specimens in a FEI Quanta 200 electron microscope at an accelerating voltage of 2–5 kV. The samples were sputter gold coated for 30 s using an Agar sputter coater. A magnification of ×100 was used for all the neat samples, and magnifications of ×500–×

1000 were used for the UV stabilized samples in order to observe the possible formation of small cracks on the surface.

FTIR spectra were obtained at room temperature using a Perkin Elmer Frontier Spectrum 400 FTIR spectrometer connected to a MIRACLE ATR detector with a ZnSe crystal. It is noted that ZnSe ATR detectors, unlike diamond or even Ge ones, do not offer optimum resolution for CB pigmented articles. Sixteen scans in the range of 4000–550 cm^{-1} were done on each sample. The CI was calculated using Equation (2).^[33]

$$CI = \frac{\text{Absorption of carbonyl species}_{1650-1800 \text{ cm}^{-1}}}{\text{Absorption of C-H peak}_{1420-1480 \text{ cm}^{-1}}} \quad (2)$$

Non-isothermal melting and crystallization analysis was performed in a PerkinElmer 8500 differential scanning calorimeter (DSC) under nitrogen atmosphere. The analysis was performed on samples of 5–10 mg. Aluminum pans were used to seal the samples, and an empty aluminum pan was used as reference. The samples were first heated from 30 to 180°C at a heating rate of 10°C/min, held at this temperature for 1 min., and cooled to 30°C at the same rate, followed by reheating to 180°C at the same rate. The melting enthalpy ΔH° and melting peak temperature (T_m) were determined from the first and second heating curves, while the crystallization temperature (T_c) and crystallization enthalpy were calculated from the cooling curve. The heat of fusion of the 100% crystalline polymer (ΔH_0) was 293 J/g.^[34,35]

Thermal decomposition was examined by using thermogravimetric analysis in a PerkinElmer TGA-4000 TGA/DSC. Approximately 15–30 mg of sample was heated from 30 to 600°C at a heating rate of 10°C/min under nitrogen atmosphere. The onset of decomposition temperature was defined as the temperature at 5 wt% mass loss ($T_{d5\%}$).

The successive self-nucleation and annealing (SSA) experiments were performed in a PerkinElmer DSC8500 DSC. The samples were heated from 0 to 180°C at 20°C/min, cooled to 0°C at 20°C/min, heated to $T_{s,id}$ at 20°C/min, held at $T_{s,id}$ for 5 min, and cooled to 0°C at 20°C/min. The samples were then successively heated to $T_{s,id}-5^\circ\text{C}$, $T_{s,id}-10^\circ\text{C}$, $T_{s,id}-15^\circ\text{C}$, $T_{s,id}-20^\circ\text{C}$, and $T_{s,id}-25^\circ\text{C}$ at 20°C/min, in each case held for 5 min, and cooled to 0°C at 20°C/min. Finally, the samples were heated to 180°C to obtain the SSA thermal fractionation curves for the LLDPE samples.

The molar weight distributions (MWD) of the samples were determined by GPC. The measurements were done in a PL 220 high-temperature size exclusion chromatograph (Polymer Laboratories, Church Stretton, UK). The temperature of the autosampler and the column compartment was set to 150°C. A mobile phase flow rate of 1 ml/min was used. For each UV sampling time,

fractured impact and/or tensile specimens were powdered, so as to prepare the solutions for GPC analysis. It is assumed that the materials are homogeneous, since samples were rotated so as to be equally exposed to UV-radiation. Polymer samples were dissolved for 4 h in TCB (containing 1 g/L butylated hydroxytoluene as stabilizer) at 160°C. A sample concentration of 2 g/L was used. 200 μl of polymer solution were injected per analysis. Each sample was analyzed twice and the results were averaged. A guard column (PLgel Olexis, 50 \times 7.5 mm [L \times I.D.]) and three analytical columns (3 \times PLgel Olexis, 300 \times 7.5 mm [L \times I.D.], with particle size 13 μm , Agilent, Waldbronn, Germany) were used for separation. An infrared detector (IR4, PolymerChar, Valencia, Spain) was used for detection. Data were collected and processed using WinGPC-software (version 7) from PSS (Mainz, Germany). Molar masses were calibrated with polystyrene (PS) standards (Polymer Standards Services, PSS, Mainz, Germany).

3 | RESULTS AND DISCUSSION

3.1 | Microscopic analysis

SEM analysis was performed to observe the surface morphology of the neat and UV/heat stabilized samples, before and after 2500 h of UV exposure (Figure 2). The main purpose was to observe the formation of cracks as a result of the UV exposure. The UV exposure caused degradation on the surfaces of both pigmented and unpigmented non-stabilized polymers, with significant cracking.^[23] LLDPE with CB shows much smaller cracks (Figure 2), proving that CB alone successfully acted as UV absorber, causing much less penetration of the UV photons into the polymer sample, as well as much less degradation of the polymer surface. A larger part of the bulk polymer therefore remained intact, which prevented increases in the crack diameter and perpendicular fracturing of the surfaces of these samples. Nevertheless, the formation of these cracks should definitely have a negative impact on the mechanical behavior of the material. An interesting observation is that for both the LLDPE without CB and the LLDPE with CB, the crack formation is unidirectional, which is probably the direction of crystal growth of the polymer during injection molding. Turning to the stabilized compounds, a significant improvement was observed in the UV1 and UV2 stabilized LLDPE samples, with and without CB (Figure 2). Even after 2500 h UV exposure, none of these samples showed any evidence of crack formation. This proves that both our HALS/UV-A formulations successfully protected the LLDPE surface from UV-initiated degradation, and therefore there was little influence on the mechanical behavior of the material is anticipated.

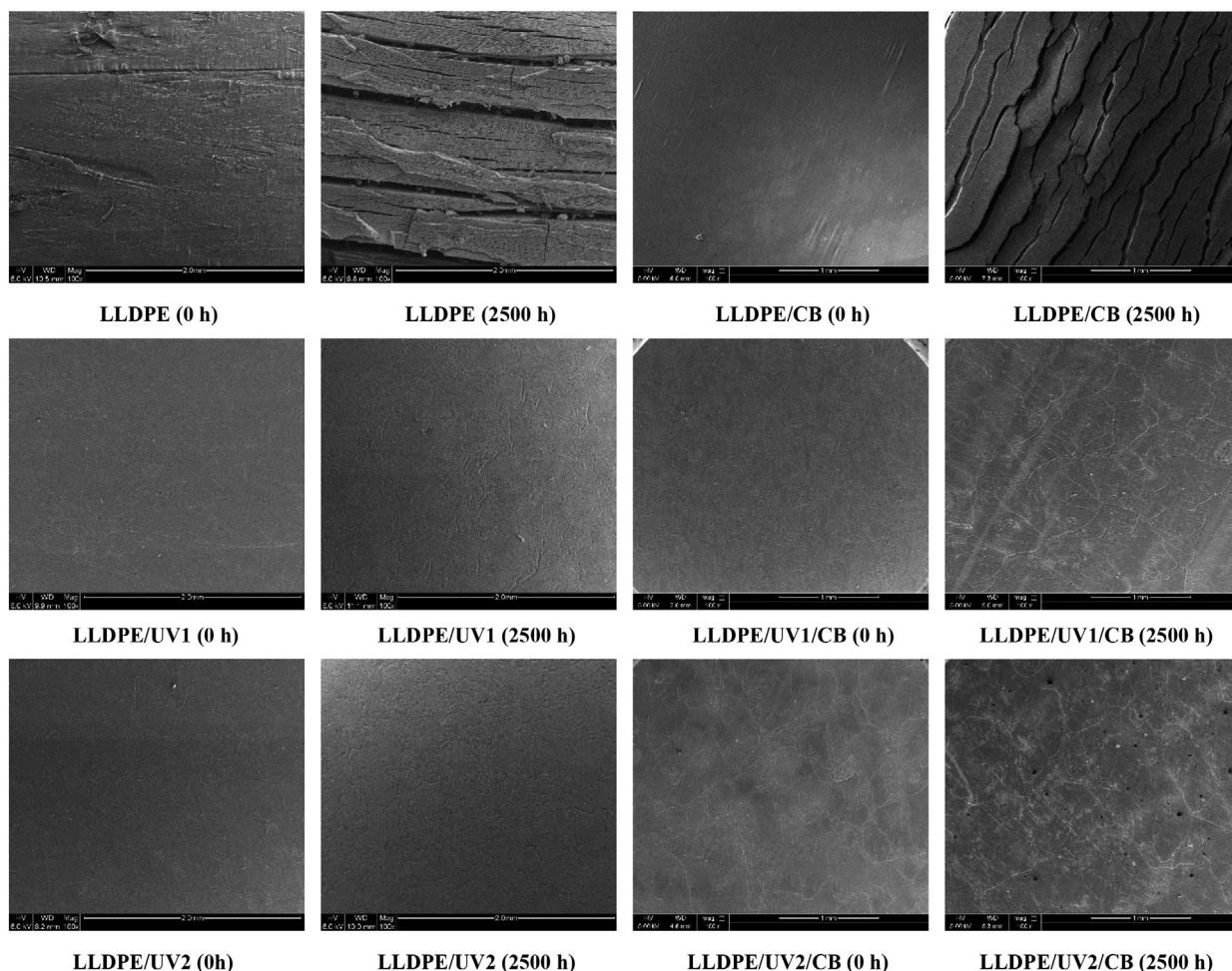
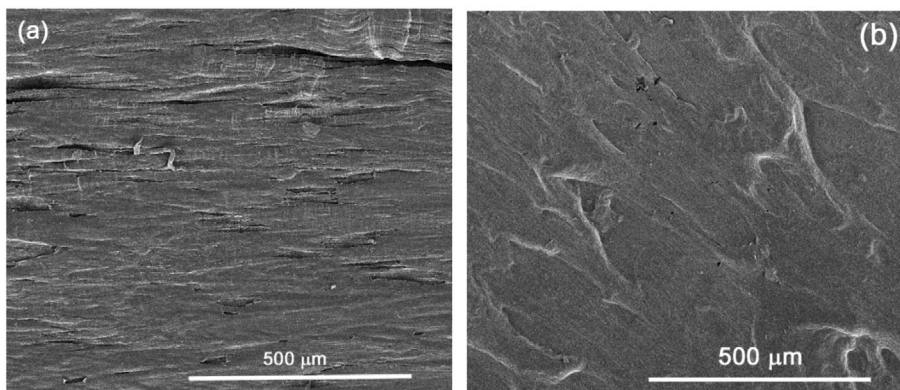


FIGURE 2 SEM images of unexposed and 2500 h UV-exposed LLDPE samples. LLDPE, linear low-density polyethylene; SEM, scanning electron microscopy

FIGURE 3 SEM images of (A) LLDPE/CB and (B) LLDPE surfaces after 12 months of heat aging. CB, carbon black; LLDPE, linear low-density polyethylene; SEM, scanning electron microscopy



The surface of the heat-aged samples (after 12 months) was also observed by SEM (Figure 3). It is also clear that the heat-induced degradation of both unstabilized LLDPE grades is much slower and less destructive than the respective UV-induced degradation, if the extent of crack formation in Figure 2 is taken into account. Moreover, it should also be noticed that heat exposure time (12 months equal to ~8800 h) was 3.5 times higher than that of UV exposure

(2500 h). Nevertheless, the heat exposed CB containing sample (Figure 3(A)) exhibits very thin cracking, unlike the surface of the respective unpigmented grade, which is almost intact (Figure 3(B)). This is expected since, CB is known to be an effective UV absorber and therefore it is the most common pigment used in the production of irrigation pipes for outdoor applications, but it is also reported to have a negative impact on the long-term

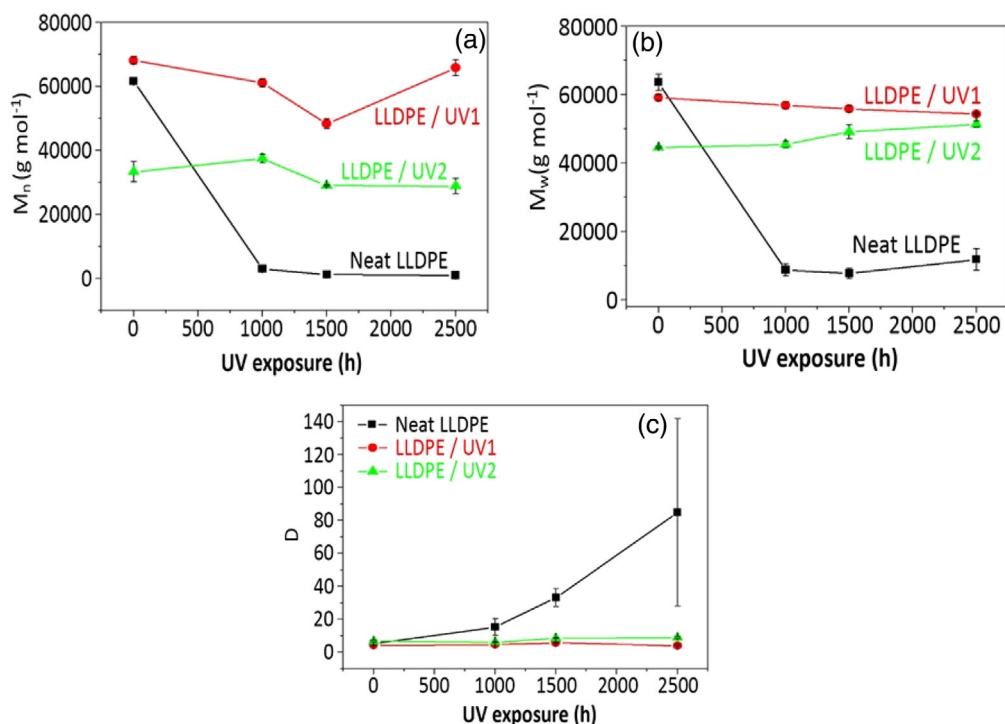


FIGURE 4 (A) Number-average MW, (B) weight-average MW, and (C) $D = M_w/M_n$ of the unpigmented LLDPE formulations. LLDPE, linear low-density polyethylene; MW, molecular weight

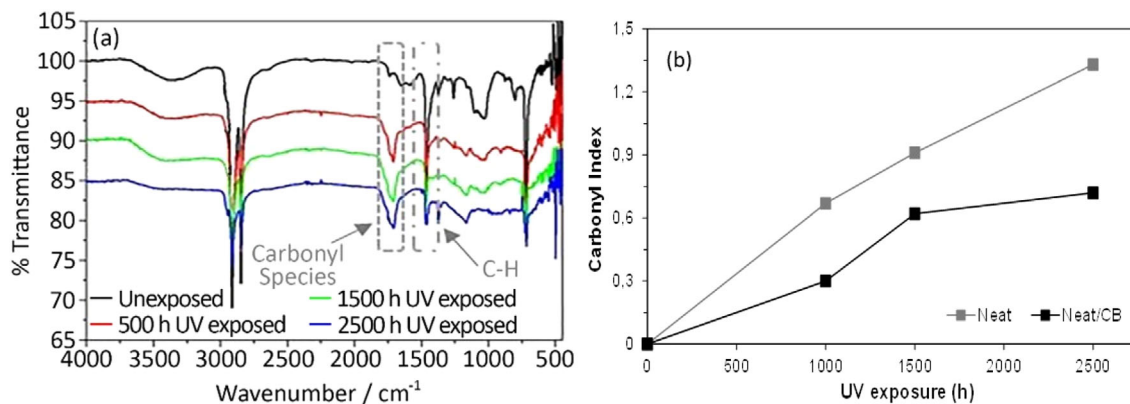


FIGURE 5 (A) LLDPE FTIR spectra after different exposure times. (B) Carbonyl index values as determined from the FTIR spectra of the unstabilized LLDPE grades. FTIR, Fourier transform infrared; LLDPE, linear low-density polyethylene

heat stability.^[36] In addition, macroscopically all pigmented neat LLDPE samples exhibited intense shrinkage during thermal aging, thus proving the negative impact of CB upon exposure to heat. The stabilized heat-aged samples were not observed by SEM, as they are expected to maintain their smooth surface, since HALS is known to contribute also to long-term thermal stability.^[15,29,32]

3.2 | MW determination

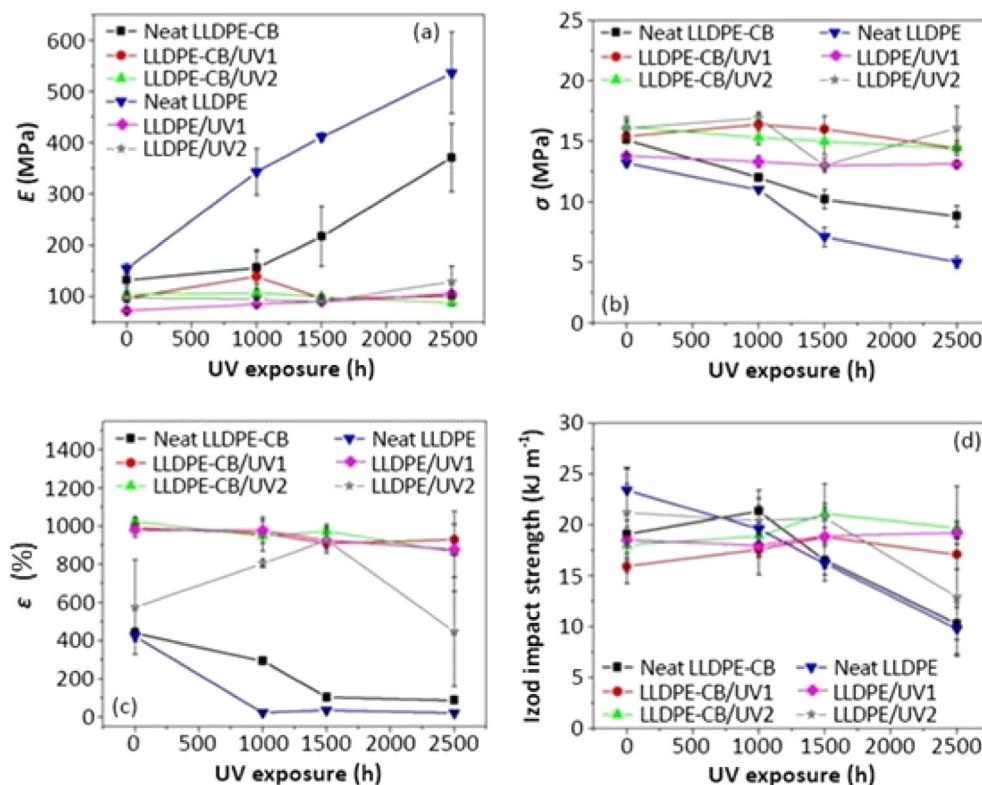
GPC was used to observe changes in the molecular weight (MW) and MW-distribution of the investigated samples as function of UV exposure time only for the

TABLE 2 Tensile properties of LLDPE grades prior to any exposure (0 h)

LLDPE samples	E (MPa)	σ_{\max} (MPa)	ϵ_{\max} (%)
Unpigmented grades			
Neat	154 ± 10	13.2 ± 0.3	424 ± 27
UV1	72.3 ± 4.8	13.8 ± 0.1	980 ± 40
UV2	97.4 ± 6.0	16.1 ± 0.9	575 ± 248
Pigmented grades			
Neat/CB	132 ± 13	15.1 ± 0.3	439 ± 27
UV1/CB	96.6 ± 8.7	15.4 ± 0.2	990 ± 30
UV2/CB	104 ± 5	16.2 ± 0.5	1024 ± 17

Abbreviations: CB, carbon black; LLDPE, linear low-density polyethylene.

FIGURE 6 (A) Young's modulus, (B) tensile strength, and (C) elongation at break and (D) Izod impact strength of the LLDPE grades as function of UV exposure time. LLDPE, linear low-density polyethylene



unpigmented LLDPE grades (Figure 4). The detailed data are also given in Table S1 in the Supplementary Section. GPC analysis was performed only for the unpigmented samples, due to the insoluble fraction of CB. For the neat LLDPE, a sharp decrease in average MWs was observed after the first 1000 h of UV exposure, which remained almost constant after longer UV exposure periods. These findings confirm that degradative chain scission occurred in the case of the unstabilized LLDPE. The chain scissions lead to an increased melt flow index and reduced MW values according to literature.^[23,34,36] It is worthwhile mentioning that the raw LLDPE material, as provided by QAPCO, is not heat stabilized (already written in the experimental part), meaning that no primary (hindered phenols) or secondary (phosphites) antioxidants were added. Consequently, there are no additives to scavenge free radicals (alkoxy, peroxy) or hydroperoxides produced during the oxidation cycle and the degradation is evolved unimpeded.^[15,32] On the other hand, the MW values changed little for the UV/heat stabilized samples, which indicates the absence of chain scission and confirms the successful stabilization of LLDPE for both formulations. In more detail (Table S1, Figure 4(C)), one may say that UV1 performed slightly better, since at 2500 h M_n was reduced by ca. 3% and M_w ca. 8%. On the contrary, for UV2 the reduction in M_n at the same time interval was 13.5%, while M_w increased by 15%, leading to an increase in D from 6.7 to 8.9. This shows that for

UV2 some minor degradation occurred. Nevertheless, in both neat and stabilized samples no obvious gel fractions were observed in the prepared solutions, meaning that crosslinking was not severe within our experimental conditions.

3.3 | FTIR spectroscopy

FTIR is a technique used to obtain information about the changes in a polymer's chemical composition after UV aging. This analysis was performed to evaluate the degree of degradation by measuring the amount of one of the major photodegradation products, the carbonyl groups. The CI was calculated from the respective intensities of the carbonyl peak ($1650\text{--}1800\text{ cm}^{-1}$) and the C—H peak ($1420\text{--}1480\text{ cm}^{-1}$) (Figure 5(A)).

Both neat unstabilized grades show peaks in the carbonyl wavenumber range, which increase in intensity with increasing UV exposure time (Figure S1 a and b in Supplementary Information). The increase in CI is, however, slower for the pigmented grade, proving that the CB slowed down the UV-initiated degradation and the consequent chain-scission, acting as a UV absorber (Figure 5 (B)). In addition, there is no clear transformation of the vinylidene band at 888 cm^{-1} to a new band (i.e., vinyl) at 909 cm^{-1} , which would imply crosslinking,^[26–28] thus the main degradation mechanism for the neat LLDPE

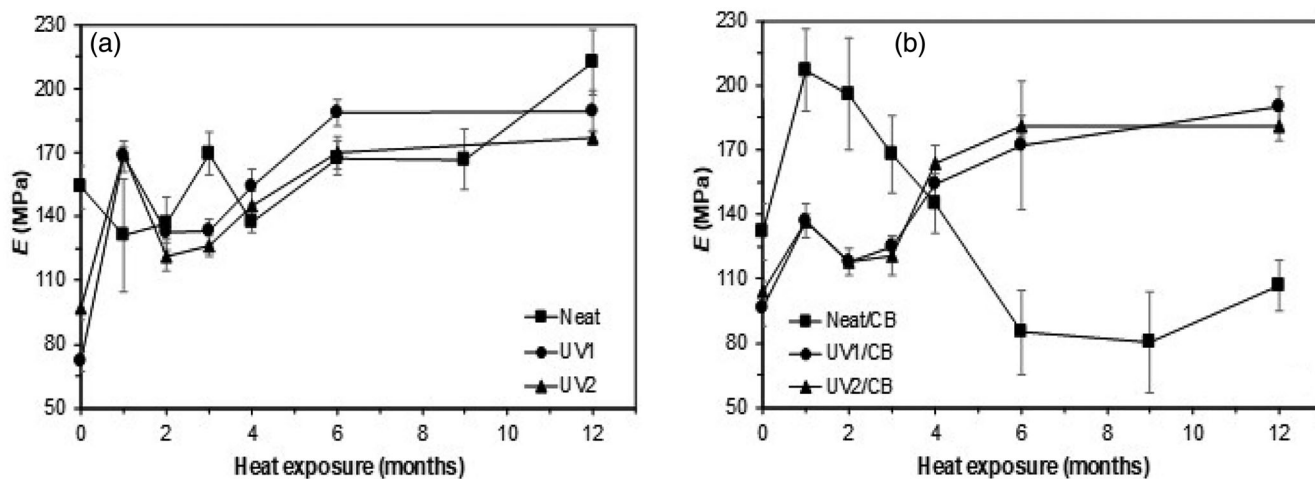


FIGURE 7 Tensile test results during heat aging (A) Young's modulus unpigmented, (B) Young's modulus pigmented

grades is chain-scission. On the contrary, all the aged stabilized compounds, with and without CB (Figure S1 c–f in Supplementary Information), showed almost no peaks or the calculated CI indices were found lower than 0.1 within the carbonyl range, indicating the successful inhibition of oxidative degradation products in these samples, which further confirms that the UV stabilizers sufficiently protected the samples from photodegradation. However, according to literature, CI is not always a reliable and accurate indication of photodegradation.^[37] This is because the oxidation process begins on the surface and free radicals propagate toward the center of the sample, leading to further degradation. Moreover, this technique does not give any information about potential deactivation or even complete loss of the photo-stabilizer. According to literature, HALS additives are being regenerated during the photo-oxidation process,^[17] but they may well be lost by evaporation and/or leaching from the polymer surfaces, thus decreasing their concentration in the compound.^[14] Such behavior can be verified in the spectra of the unpigmented UV1 and UV2 grades by the peak at $\sim 1100\text{ cm}^{-1}$ and 1534 cm^{-1} (Figure S1 c and e in Supplementary Information), which corresponds to the HALS components.^[14,26–28] The particular peak is strong at 0 h for both compounds and remains visible almost at the same intensity up to 1500 h for UV1 and 1000 h for UV2, showing that the HALS component is still active and regenerated during the stabilization process. Furthermore, it is also proven that HALS1 shows higher durability than HALS2 for the unpigmented grades. Subsequently, at 2500 h no peak is detected for both compounds, probably meaning that the HALS additive is lost or deactivated. In the case of the pigmented LLDPE grades, even though that the used ZnSE ATR detector is not ideal for CB pigmented articles,

(Figure S1 d and f in Supplementary Information), the performance of the formulations seems reversed with UV2/CB compound showing in overall higher durability since the peak at $\sim 1100\text{ cm}^{-1}$ is observed constantly up to 2500 h. Thus, the superior performance of HALS2 in the presence of CB is verified.^[15] Furthermore, CB also seems to enhance the durability of HALS1 also, since at 2500 h a weak peak is also observed at the pertinent region, meaning that some HALS is still active.

3.4 | Determination of mechanical properties

3.4.1 | Tensile testing

Tensile testing was firstly performed on all the LLDPE samples prior to any aging (0 h, Table 2). According to the obtained results of the unpigmented grades, the incorporation of 0.2 wt% HALS and UV-A additives resulted in significantly decreasing the Young's modulus (E) in both formulations from 154 MPa in the neat polymer to 72 and 97 MPa in UV1 and UV2 respectively. This along with the simultaneous increase in ϵ_{max} show that the material became softer and more ductile. Similar behavior was observed for the pigmented grades; however, the determined decrease was milder. Turning to the maximum tensile strength (σ_{max}) of the unpigmented grades was found similar ($\sim 13.5\text{ MPa}$) for neat and UV1, but increased to 16 MPa for UV2. Neat/CB and UV1/CB exhibited similar values ($\sim 15\text{ MPa}$), but were found increased compared to the respective unpigmented grades. UV2/CB showed the same σ_{max} value with UV2. As far as the elongation at break (ϵ_{max}) is concerned, the value for the neat polymer was 474%, while increased

values of 980% and 575% were recorded for UV1 and UV2 respectively. Finally, the neat CB pigmented LLDPE showed similar elongation value to the respective unpigmented grade, while sharp increases were also determined for UV1/CB and UV2/CB (990% and 1024% respectively).

Turning to the tensile properties of the UV-aged LLDPE compounds (Figure 6, Table S2 in Supplementary Information), it is clear that the tensile strength and elongation at break of the neat LLDPE decreased significantly with increasing UV exposure time, which is in line with the SEM and FTIR results, and with other results reported in literature.^[1,33] Both neat compounds with and without CB (Figure S2 in Supplementary Information) show a decrease in tensile strength of up to 60%, accompanied with a similar reduction in elongation, as a function of UV exposure time. In literature, the reduction

in strain at break is related to embrittlement as a result of chain scissions on the polymer lattice, but simultaneously, crosslinking may occur.^[1,33] The reduction in the values of the tensile strength and strain at break was less significant in the CB pigmented LLDPE samples, which supports the given explanation for the differences in surface topography in Sections 3.1 and 3.3. The Young's modulus (E) values increased significantly for both unstabilized LLDPE grades with increasing UV exposure time, but this was not the result of polymer reinforcement, as it increased at the expense of ductility.^[12,23,25,33,38] The increase was much more significant for the unpigmented grade (4.5-fold increase), which obviously enabled more intense UV-initiated chain scission. On the contrary, for the pigmented grade, once again CB alone was proven to protect the polymer matrix from UV radiation to some extent, acting as UV absorber. It is also known that the more linear PE grades are, they get more susceptible to crosslinking reactions during weathering,^[39] which is why we should not exclude the contribution of minor UV-initiated crosslinking to the increase in sample stiffness, although it was not observed via gel fractions during the preparation of the GPC solutions. The Young's modulus seems as more consistent and accurate value for evaluating the behavior of the material upon aging within our experimental conditions, since tensile strength and elongation and break exhibit intermediate variations and not always clear trends.

Turning to the stabilized compounds, the tensile strength and elongation at break values of the stabilized LLDPE with and without CB were higher than those of the unstabilized LLDPE samples, and changed little within experimental error with increasing UV exposure

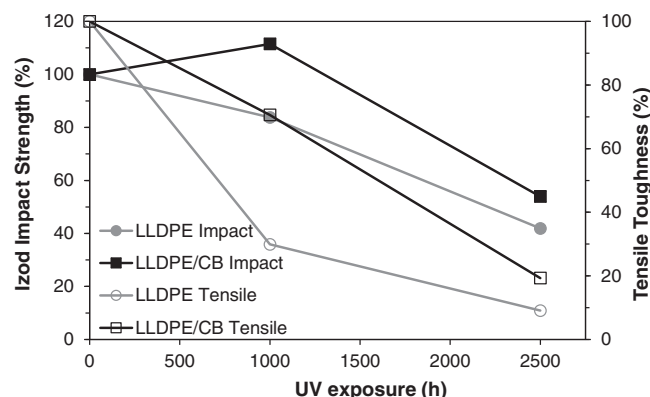


FIGURE 8 Comparison between Izod impact strength and tensile toughness for UV-aged LLDPE and LLDPE/CB. CB, carbon black; LLDPE, linear low-density polyethylene

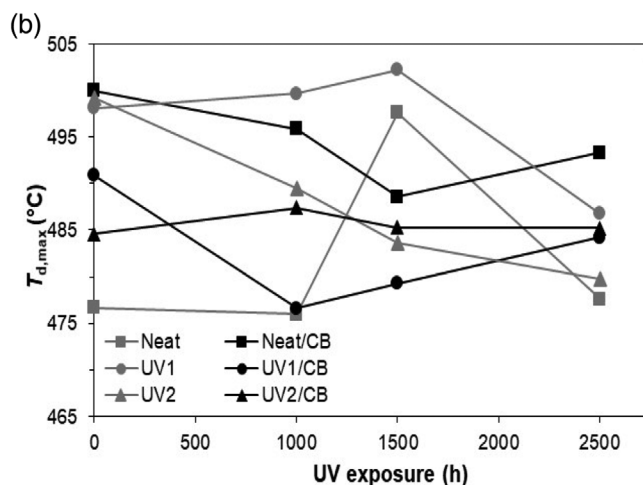
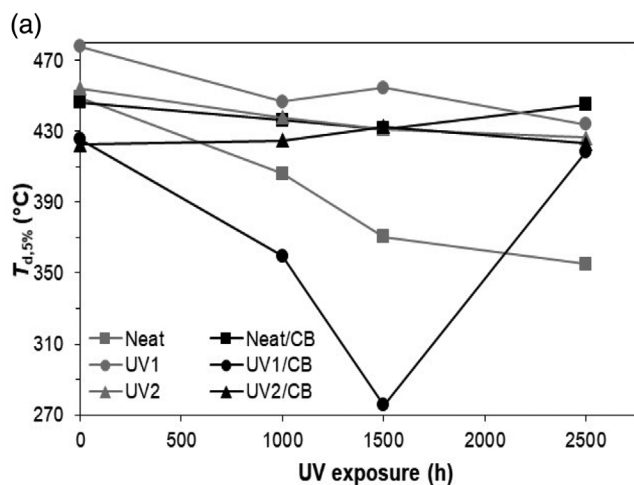


FIGURE 9 TGA results as a function of UV exposure time for pigmented and unpigmented LLDPE grades. (A) $T_{d,5\%}$, (B) $T_{d,max}$. LLDPE, linear low-density polyethylene

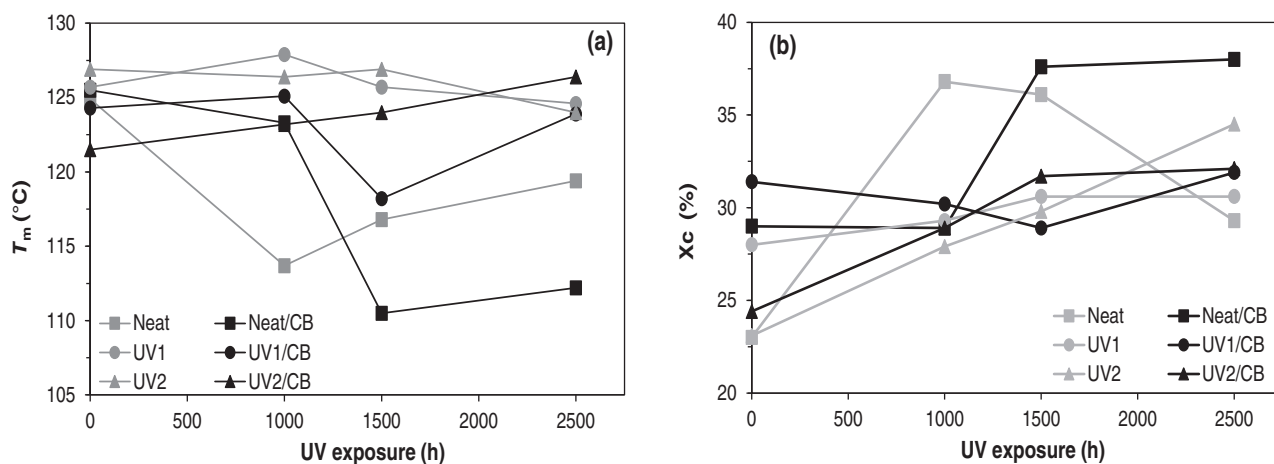


FIGURE 10 DSC results as a function of UV-aging time (A) melting point and (B) crystallinity. DSC, differential scanning calorimeter

time (Figure 6(B),(C)), implying successful stabilization. There is also little difference between these values for the LLDPEs with and without CB, which is an indication that the HALS and UV-A additives played a much more prominent role in stabilizing the LLDPE against UV initiated degradation. It is observed that the tensile strength and strain at break values for UV2 are significantly scattered with relatively large standard deviations. The Young's modulus value, which is the most consistent property, of the pigmented stabilized compounds during UV exposure did not change significantly with increasing aging time. However, in the case of the unpigmented grades, UV1 showed a continuous increase of $\sim 46\%$ from 0 to 2500 h, while in the case of UV2, the latter was constant up to 1500 h, but at 2500 h showed a sharp increase of $\sim 32\%$, but with a high deviation. This proves that the incorporation of CB enhances UV stabilization, since the pigment acts as an additional UV absorber. Nevertheless, in both cases, the performance of all the stabilized compounds during aging was much better than those of the neat polymers, and therefore the HALS/UV-A additives used in this work successfully protected the LLDPE against UV initiated degradation, even when used at the lowest recommended concentrations. In overall, UV1 seems to perform slightly better especially among the unpigmented compounds.

Tensile testing was also performed on the heat-aged samples. Thermal aging at 100°C was additionally performed for up to 12 months (~ 8800 h) so to exclusively study the effect of an extremely hot environment on the mechanical behavior of the LLDPE based samples. The UV aging investigation was also performed between 50 and 60°C , which is milder than 100°C , but in that investigation the effect of UV radiation was predominant. In the case of thermal aging the HALS additives are expected to perform also as long-term heat stabilizers by

scavenging the radicals formed during heat aging.^[14–16,40] For the heat aging experiments only the Young's modulus is used to evaluate the mechanical behavior as a more consistent value (Figure 7), nevertheless all received tensile data are given also in Table S2 (Supplementary Information). Accordingly, the unpigmented neat LLDPE (Figure 7(A)) showed a mild decrease in Young's modulus of $\sim 15\%$ after the first month of exposure, while after the same time interval the respective pigmented sample showed a sharp increase of $\sim 57\%$. In the specific time interval, the pigmented grade showed intense embrittlement (Figure 7(B)), probably due to crosslinking. The latter is reported in literature for LLDPE,^[41] and clearly proves the negative impact of CB on heat aging.^[40] Subsequently, during the rest of the aging time, the unpigmented grade slowly tended to embrittlement, since from 3 to 12 months of exposure the Young's modulus gradually increased to 212 MPa (overall increase of $\sim 38\%$). On the contrary, the respective value of neat/CB significantly increased during the first 2 months of thermal exposure, and then continuously decreased from 196 MPa after the second month to 107 MPa after the twelfth month, showing an overall decrease of 19% from its initial value. It could be that heat energy is more easily absorbed in the presence of CB, which would have accelerated the thermal degradation process.^[40]

As far as the tensile results of the stabilized unpigmented LLDPE grades during heat aging are concerned (Figure 7(A), Table S3), both UV1 and UV2 performed similar in terms of Young's modulus. Both formulations showed a sharp increase during the first month of exposure with E increasing to ~ 169 MPa ($\sim 133\%$ and $\sim 74\%$ increase for UV1 and UV2 respectively). This behavior was also observed for the neat grade, but only after 3 months of exposure. Annealing is very common during heat aging, resulting in increased

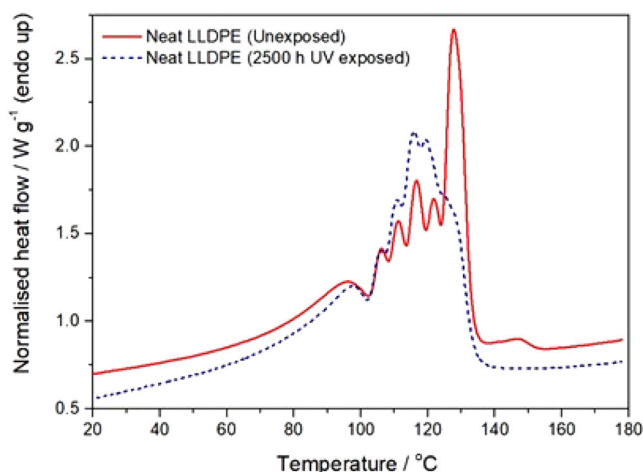


FIGURE 11 SSA curves for neat LLDPE (unexposed and 2500 h UV exposed). LLDPE, linear low-density polyethylene; SSA, successive self-nucleation and annealing

crystallinity and consequently increased Young's modulus and tensile strength.^[26–28,41,42] Here it seemed as if the annealing effect occurred much earlier for both stabilized grades. However, in both cases, the Young's modulus values at 12 months of exposure of both UV1 and UV2 are lower than the respective value of the neat grade, showing that the HALS additives limited the heat-induced degradation to some extent. Turning to the pigmented grades (Figure 7 (B)), UV1/CB and UV2/CB follow exactly the same trend. One may say that both unpigmented stabilized compounds also tend to embrittlement but it seems to be much slower than neat/CB sample due to increased annealing at the beginning of the aging, which could have prevented or decelerated thermal degradation.

3.4.2 | Impact testing

Izod impact testing was conducted to measure the impact strength of the samples, which gives more information about their toughness. Measurements were performed on the neat and UV/heat stabilized samples, only for the UV-aged samples (Figure 6(D)). Regarding the unpigmented samples prior to UV aging, it seems that the neat LLDPE is the most impact resistant material with an impact strength of ~ 23 kJ/m², followed by UV2 (21 kJ/m²), with the lowest impact strength determined for UV1 (18.5 kJ/m²). The trend remains the same for the unexposed pigmented materials, but the values are slightly lower than those of the respective unpigmented grades, proving that the addition of 0.3 wt% CB influenced the impact behavior of the materials, which was also observed in the tensile properties. Neat and neat/CB samples showed a 58% and 46% decrease in the Izod impact strength after UV exposure, while the stabilized

compounds showed little or no decrease. This is in line with the previously presented GPC and tensile data and is attributed to the severe degradation of neat LLDPE. UV1 and UV1/CB showed almost no change in the Izod impact strength with increasing UV aging time. This indicates that the used stabilizers almost completely prevented degradation during UV-aging. The impact strength of UV2 remained constant up to 1500 h UV exposure, but then decreased significantly ($\sim 40\%$) after 2500 h of UV exposure. On the other hand, UV2/CB showed no change in impact strength with increasing UV exposure time. This is in complete agreement with the aforementioned FTIR analysis, where HALS2 was not detected in the spectra at 2500 h for the unpigmented grade, while the presence of CB enhanced the UV stability of this particular formulation.

In addition, the tensile toughness was calculated from the stress strain curves (area below the curves in Figure S1 in Supplementary Information) and was compared to the Izod Impact strength, only for the case of LLDPE and LLDPE/CB. Nevertheless, in order to compare values of tensile toughness (kJ/m³) with the respective of Izod impact strength (kJ/m²), a transformation to percentage variation from the unexposed sample (0 h) was applied (Figure 8). This means that at 0 h Izod impact strength and tensile toughness is at 100% for all samples. At 2500 h for LLDPE reduce to 41% is recorded for the impact strength, while a much sharper decrease to 9% was calculated for the tensile toughness. On the contrary, for LLDPE/CB, the respective values at 2500 h are 54% and 19%, proving once again that CB alone protected the LLDPE matrix to some extent from UV-induced degradation.

All the UV aging results indicate that the UV1 formulation performed better than the UV2, although the UV-A2 is known for its much higher UV absorbing efficiency. One reason could be that the benzophenone type UV absorber (UV-A1) has a melting point just below 50°C, and can therefore be easily dispersed. On the contrary, UV-A2 (hydroxyphenyltriazine type) melts at $\sim 150^\circ\text{C}$ and consists of a six-carbon side chain known for its strong hydrogen bonding, in contrast to UV-A1 (8-carbon side chain) (Figure 1). Taking all these reasons into consideration it might also be that the absorber capacity of UV2 could not be fully exploited. However, in the presence of CB, UV2/CB shows improved performance and in overall somewhat better than UV1/CB.

3.5 | Thermal analysis

3.5.1 | Thermogravimetric analysis

The thermal decomposition behavior of the UV-aged samples was studied through TGA analysis (Figure S3,

Table S4 in Supplementary Information). The onset of degradation, which was determined as the temperature at 5% mass loss ($T_{d,5\%}$) (Figure 9(A)), and the degradation temperature ($T_{d,max}$), which is the temperature at the maximum mass loss rate (determined from the peak maxima in the dTGA curves), were used to monitor the thermal stability of the polymer (Figure 9(B)). Regarding the LLDPE compounds prior to any exposure, the $T_{d,5\%}$ and $T_{d,max}$ values were 449 and 477°C for the neat sample, and 446 and 500°C for LLDPE/CB. The thermal decomposition started at similar temperatures, but the presence of CB seemed to slow down the thermal degradation by absorbing the heat. For the stabilized compounds, the $T_{d,5\%}$ and $T_{d,max}$ values at 0 h increased by 29 and 21°C for UV1, and by 5 and 22°C for UV2. It is obvious that the used additives were also effective at high temperatures, by shifting the degradation to higher temperatures, since the HALS compounds can neutralize the formed radicals and the UV-A can absorb heat. On the contrary, in the case of the pigmented grades, the interference of the UV/heat additives with CB at 0 h seemed to have had a negative impact on the thermal stability of the particular compounds. Accordingly, the $T_{d,max}$ values reduced by 9 and 14°C for UV1/CB and UV2/CB respectively, while the decrease in $T_{d,5\%}$ was even higher, that is, 21 and 24°C.

Turning to the thermal stability during UV aging (Figure 9), the $T_{d,max}$ value of the neat LLDPE is practically constant at ca. 477°C after 2500 h of exposure. However, $T_{d,5\%}$ decreases by 94°C from 0 to 2500 h, which is in agreement with the intense MW decrease determined from GPC in Section 3.2. Turning to the neat/CB, the decrease in $T_{d,5\%}$ was limited to ca. 15°C at 1500 h and then returned to 445°C at 2500 h. This shows that CB decelerated the UV-induced degradation, by absorbing part of the UV radiation, which is also in agreement with the milder surface degradation observed in Section 3.1 and the slower embrittlement determined in Section 3.4.1. Regarding the stabilized compounds, UV1 showed an irregular decrease in $T_{d,5\%}$ (ranging from ~23 to 44°C), while for UV2 a clear decreasing trend was observed, reaching 426°C (~28°C lower than that for the unexposed sample) at 2500 h. A constantly decreasing trend was also observed for the $T_{d,max}$ values of UV2 (~20°C lower after 2500 h), while in the case of UV1 it increased slightly up to 1500 h, and then decreased by ~11°C for the 2500 h exposed sample. The thermal stability as a function of UV aging time, for both UV1 and UV2, is not in line with changes in the MW of the specific samples, which changed very little during UV aging, as determined by GPC in Section 3.2. In view of this, the aged samples should have deviated less from the unexposed ones. Still, both stabilized compounds

performed better than the neat polymer in terms of thermal stability, with UV2 showing a slightly better retention of $T_{d,5\%}$, while UV1 shows a better retention of $T_{d,max}$. Similar conclusions can be drawn for the thermal stability results of the pigmented grades, where again not always clear trends were observed. A plausible explanation is that the samples contained both degraded (surface) and non-degraded (bulky) polymer fractions, since the degradation might not have penetrated deep enough during the applied exposure periods, although the specimens were rotated in the weathering machine. In overall, UV2/CB showed better retention of the thermal stability among the pigmented grades.

3.5.2 | Differential scanning calorimetry

Beginning with the DSC results (Figure S4, Table S5 in Supplementary information) of the LLDPE compounds prior to any aging, it seems that both neat grades have very similar melting points (T_m) of ~125°C, but the enthalpy of neat/CB is much higher than that of the unpigmented one, probably because the CB acts as a nucleating agent. As far as the stabilized compounds are concerned, UV1 shows similar T_m to the neat LLDPE, but again enthalpy values are significantly higher, while UV2 shows ~2°C higher T_m . ΔH_m ; however, are the same as those of the neat polymer. The respective pigmented compounds show reduced T_m values, especially for UV2/CB where the T_m was 4°C lower, but their enthalpies were much higher (especially for UV1/CB) than the neat and the respective unpigmented stabilized grades. Nevertheless, the main aim of this analysis was to understand the effect of UV degradation on the thermal properties of the investigated samples. Only the first heating curves are reported (Figure S4 in Supplementary information), so as to focus on the thermal history as imposed by the UV radiation, otherwise after melting the cooling curves and crystallization peaks would have been averaged out.

According to the first heating curves of the unstabilized grades (Figure 10(A),(B)) it is obvious that in the absence of the UV protection additives, there was degradative chain scission and recrystallization during UV exposure, which led to lower melting temperatures (because of the formation of smaller crystals after recrystallization of the shorter chains formed as a result of degradative chain scission), and higher degrees of crystallinity because it was easier for the shorter chains to rearrange into a crystalline morphology. The unpigmented neat grade (Figure 10(B)) shows a rapid increase in X_c from 0 h (ca. 23%) to 1000 h (ca. 37%), due to increased annealing of the fragmented chains, completely in line with the GPC results at the same time interval.

Subsequently, remains almost constant up to 1500 h (ca. 36.1%), but decreases significantly to 29% at 2500 h. On the contrary, the presence of CB seems to have delayed this behavior, since both T_m and crystallinity are almost the same up to 1000 h. Subsequently, X_c increases to ca. 38% with the degradation being evident in the neat LLDPE/CB SEM images in Figure 2.

For the aged stabilized compounds, UV1 seemed to be very effective against UV radiation, because both the melting temperatures and crystallinity values did not change significantly in the absence and presence of CB, indicating that very little UV initiated degradation occurred in these samples. On the other hand, the unpigmented UV2 shows almost no change in melting temperature, but a clear increase in X_c with increasing UV exposure time (Figure 10(B), Table S5 in Supplementary information). This could only be the result of annealing, since the GPC results showed almost no change in MW. In UV2/CB this behavior gets even more pronounced, since an increase in T_m values up to 5°C was observed. Similar remarks can be observed also in the case of the cooling curves (Table S4, Figure S5 in Supplementary information).

To further support the discussion above, we performed thermal fractionation or SSA experiments on two samples investigated in this paper. The SSA curve for the unexposed neat LLDPE (Figure 11) shows a number of crystal fractions, with the main fraction in the temperature range 130–140°C. This indicates that the main fraction consists of fairly large crystals. The SSA curve for the 2500 h UV-exposed sample is completely different from that of the unexposed LLDPE. This curve also shows a number of crystal fractions, but they are much less clearly resolved, and the most intense fractional peaks fall within a much lower temperature range of 110–120°C. This is a clear indication of the chain scission that occurred during the UV initiated degradation of the sample, and is in line with all the other results.

We tried to apply the same SSA method to the UV1 and UV2 samples in order to see whether the addition of the HALS/UV-A inhibited the observed chain scission. As it can be seen in Figure S6 in Supplementary Information, both the cooling and heating curves after annealing show multiple peaks, and it was therefore not possible to identify the self-nucleation domain in order to construct proper SSA curves for these formulated samples. Nonetheless, the cooling and heating curves for the unexposed and the 2500 h UV exposed are almost identical for LLDPE/UV1 and LLDPE/UV2 respectively, thus one may reasonably assume that UV exposure did not change the fractional morphology of LLDPE for these

formulations, since no significant chain-scission occurred according to previous SEC analysis.

4 | CONCLUSIONS

The article focuses on two UV/heat stabilizer systems, without and with CB incorporated into LLDPE to be used in thick sections such as irrigation pipes, where the neat LLDPE and the LLDPE UV/heat stabilized compounds were separately exposed to accelerated UV- and heat-aging. SEM analysis of the UV-exposed neat LLDPE revealed more severe surface cracking than the pigmented LLDPE, while the aged stabilized LLDPE compounds (with and without CB) showed no obvious surface degradation. The degradative crack formation was less visible in the case of the thermally aged neat LLDPE samples, proving that heat-induced degradation is slower. The MW significantly decreased with increasing UV exposure time for the neat UV-exposed LLDPE, while both UV1 and UV2 showed insignificant change in MW, thus stabilization was successful. The tensile testing, impact testing, thermal analysis, and CI results all support the morphological results, which confirms that CB alone slightly improved the resistance of LLDPE against UV initiated degradation, but it was found to enhance the thermal initiated degradation. The UV1 and UV2 formulations were both very good at protecting the LLDPE against UV-initiated degradation for both pigmented and unpigmented grades, with UV1 being slightly more effective for the unpigmented grades and UV2 better for the pigmented ones. Furthermore, as far as heat aging is concerned, the stabilized compounds were effective only in the case of the pigmented grades, where both UV1/CB and UV2/CB successfully prevented the severe degradation induced by the pigment in the neat grade. In the case of the heat exposed unpigmented grades, little influence of the UV/heat additives was observed in terms of tensile properties. In conclusion, our combinations of HALS- and UV absorber additives had a much more significant effect on the UV-stabilization of LLDPE than on the heat stabilization, at least for the selected aging programs and temperatures. The findings are important prerequisites to provide protection of LLDPE in thick sections against intensive UV irradiation and heat aging and to develop sustainable plastic applications such as irrigation pipes in desert regions at very low concentrations. Finally yet importantly, the systems have been already combined with halogen-free flame-retardants to demonstrate excellent flame resistance in addition to long-term weathering stability.

ACKNOWLEDGMENTS

This publication was made possible by the NPRP award (NPRP 9-161-1-030) from the Qatar National Research Fund (a member of The Qatar Foundation). We are also grateful to BASF and Sabo for supplying the additives at no cost. We further express our gratitude to Dr. Robert Brüll from Fraunhofer LBF, Darmstadt, Germany for doing the GPC analyses on our samples. The statements made herein are solely the responsibility of the author(s).

DATA AVAILABILITY STATEMENT

The data that support the findings of this study are openly available in the Supporting Information section.

ORCID

Athanasios D. Porfyrus  <https://orcid.org/0000-0001-5194-4480>

Adriaan S. Luyt  <https://orcid.org/0000-0002-2766-8604>

REFERENCES

- [1] H. J. Jeon, M. N. Kim, *Eur. Polym. J.* **2014**, *52*, 146.
- [2] A. J. Peacock, *Handbook of Polyethylene: Structures, Properties and Applications*, CRC Press, Boca Raton, Florida, USA **2000**.
- [3] <http://www.prnewswire.com/news-releases/polyolefins-market-consumption-worth-1698924-kilotons-by-2018-222655431.html> (**2018**).
- [4] A. A. Basfar, K. M. I. Ali, *Polym. Degrad. Stab.* **2006**, *91*, 437.
- [5] A. Dehbi, A. H. I. Mourad, A. Bouaza, *Proc. Eng.* **2011**, *10*, 466.
- [6] J. V. Gulmine, P. R. Janissek, H. M. Heise, L. Akcelrud, *Polym. Degrad. Stab.* **2003**, *79*, 385.
- [7] Y. C. Hsu, R. W. Truss, B. Laycock, M. P. Weir, T. M. Nicholson, C. J. Garvey, P. J. Halley, *Polymer* **2017**, *119*, 66.
- [8] M. Liu, A. R. Horrocks, *Polym. Degrad. Stab.* **2002**, *75*, 485.
- [9] S. M. Al-Salem, G. Abraham, O. A. Al-Qabandi, A. M. Dashti, *Polym. Test.* **2015**, *46*, 116.
- [10] D. Rasouli, N. T. Dintcheva, M. Faezipour, F. P. LaMantia, M. R. Mastro Farahani, M. Tajvidi, *Polym. Degrad. Stab.* **2016**, *133*, 85.
- [11] <http://dohanews.co/qatar-dumps-400-tons-waste-daily-landfill> (**2018**).
- [12] S. M. Al-Salem, *Mater. Des.* **2009**, *30*, 1729.
- [13] B. Y. Zhao, X. W. Yi, R. Y. Li, P. F. Zhu, K. A. Hu, *J. Appl. Polym. Sci.* **2003**, *88*, 12.
- [14] M. Scoptoni, S. Cimmino, M. Kaci, *Polymer* **2000**, *41*, 7969.
- [15] P. Gijssman, *Polym. Degrad. Stab.* **2017**, *145*, 2.
- [16] C. E. Wilen, R. Pfaendner, *J. Appl. Polym. Sci.* **2013**, *129*, 925.
- [17] C. Jasso-Gastinel, J. M. Kenny Eds., *Modification of Polymer Properties*, Elsevier, Cambridge, MA 02139, USA **2017**, p. 87.
- [18] J. S. Carpenter, C. Bai, J. Pablo Escobedo-Diaz, J.-Y. Hwang, S. Ikhmayies, B. Li, J. Li, S. Neves, Z. Peng, M. Zhang Eds., *Characterization of Minerals, Metals, and Materials*, Springer, Cham, Switzerland **2015**.
- [19] V. Dobrescu, G. Andrei, C. Andrei, *Eur. Polym. J.* **2000**, *24*, 289.
- [20] M. Edge, J. M. Peña, C. M. Liauw, B. Valange, N. S. Allen, *Polym. Degrad. Stab.* **2002**, *72*, 259.

- [21] W. Focke, P. Mashele, N. Nhlapo, J. Vinyl, *Addit. Technol.* **2011**, *21*, 129.
- [22] K. Cristofoli, R. N. Brandalise, M. Zeni, *J. Food Process. Technol.* **2012**, *3*, 166.
- [23] A. S. Luyt, S. Gasmi, S. S. Malik, R. M. Aljindi, M. Ouederni, S. N. Vouyiouka, A. D. Porfyrus, R. Pfaendner, C. D. Papaspyrides, *Express Polym. Lett.* **2021**, *15*(2), 121.
- [24] F. Gugumus, *Polym. Degrad. Stab.* **2002**, *75*, 309.
- [25] F. P. LaMantia, N. T. Dintcheva, V. Malatesta, F. Pagani, *Polym. Degrad. Stab.* **2006**, *91*, 3208.
- [26] M. I. Babaghayou, A.-H. I. Mourad, V. Lorenzo, M. U. de la Orden, J. M. Urreaga, S. F. Chabira, M. Sebaa, *Mater. Des.* **2016**, *111*, 279.
- [27] M. I. Babaghayou, A.-H. I. Mourad, V. Lorenzo, S. F. Chabira, M. Sebaa, *Polym. Test.* **2018**, *66*, 146.
- [28] M. I. Babaghayou, A.-H. I. Mourad, N. Cherupurakal, *Advances in Science and Engineering Technology International Conferences, ASET* **2020**.
- [29] A. D. Porfyrus, S. N. Vouyiouka, A. S. Luyt, D. M. Korres, S. S. Malik, S. Gasmi, M. Grosshauser, R. Pfaendner, C. D. Papaspyrides, *J. Appl. Polym. Sci.* **2021**, *138*(19), 50370.
- [30] U. Braun, V. Wachtendorf, A. Geburtig, H. Bahr, B. Schartel, *Polym. Degrad. Stab.* **2010**, *95*, 2421.
- [31] D. Chantegraille, S. Morlat-Therias, J. L. Gardette, *Polym. Degrad. Stab.* **2010**, *95*, 274.
- [32] R. Pfaendner, *Polym. Degrad. Stab.* **2013**, *98*, 2430.
- [33] Y. C. Hsu, M. P. Weir, R. W. Truss, C. J. Garvey, T. M. Nicholson, P. J. Halley, *Polymer* **2012**, *53*, 2385.
- [34] D. M. Simpson, G. A. Vaughan, *Ethylene polymers, LLDPE. Encyclopedia of Polymer Science and Technology*, John Wiley & Sons, Inc., New York, USA **2002**, p. 441.
- [35] J. Molefi, A. Luyt, I. Krupa, *Thermochim. Acta* **2010**, *500*, 88.
- [36] D. Price, R. Horrocks, in *Fire Retardancy of Polymeric Materials*, 2nd ed. (Eds: C. Wilkie, A. Morgan), Elsevier, Amsterdam **2010**.
- [37] G. Wypych, *Handbook of UV Degradation and Stabilization*, Elsevier, Amsterdam **2015**.
- [38] T. Ojeda, A. Freitas, K. Birck, E. Dalmolin, R. Jacques, F. Bento, F. Camargo, *Polym. Degrad. Stab.* **2010**, *96*, 703.
- [39] M. Tolinski, in *Additives for Polyolefins*, 2nd ed. (Ed: M. Tolinski), Elsevier, Amsterdam **2015**.
- [40] H. Zweifel, *Plastics Additives Handbook*, 5th ed., Hanser Publishers, Munich, Germany **2001**, p. 57.
- [41] J. Weon, *Polym. Degrad. Stab.* **2010**, *95*, 14.
- [42] C. N. Kartalis, C. D. Papaspyrides, R. Pfaendner, K. Hoffmann, H. Herbst, *Polym. Eng. Sci.* **2001**, *41*(5), 771.

SUPPORTING INFORMATION

Additional supporting information may be found online in the Supporting Information section at the end of this article.

How to cite this article: A. D. Porfyrus, A. S. Luyt, S. Gasmi, S. S. Malik, R. M. Aljindi, M. Ouederni, S. N. Vouyiouka, R. Pfaendner, C. D. Papaspyrides, *SPE Polymers* **2021**, *2*(4), 336. <https://doi.org/10.1002/pls2.10055>